Strong electric-field effects on the structure profiles of doubly excited resonances in He ground-state photoionization

T. K. Fang and Y. K. Ho
Institute of Atomic and Molecular Sciences, Academia Sinica, P.O. Box 23-166, Taipei, Taiwan 106, Republic of China
(Received 20 January 1999; revised manuscript received 29 April 1999)

Electric-field effects on the doubly excited resonant structures in He ground-state photoionization are investigated theoretically using the complex-rotation method with a *B*-spline-based configuration interaction basis. Angular-momentum states up to $L_{\max}=3$ are coupled together by the external electric field for the final states. The variations of the structure profiles for the $M_L=0$ components of He $(2,5a)$ and $(2,6a)$ $^1P^o$ and $^1D^e$ resonances for selected dc electric-field strengths are examined. The changes of the resonant energies and widths are also presented. [S1050-2947(99)05009-X]

PACS number(s): 32.80.Dz, 32.80.Fb, 32.60.+i

I. INTRODUCTION

With recent high-resolution intense light sources, the doubly excited Rydberg series of He has been observed and resolved in photoionization experiments [1,2]. Parallel to the fast growing experimental techniques, significant progress has also been made in the theoretical calculations [3–5].

This work presents the photoionization of He in the energy regions of the $(2,5a)$ and $(2,6a)$ $^1P^o$ resonances under the presence of external electric fields. Electric-field effects on such $^1P^o$ states, to our knowledge, have not been investigated either theoretically or experimentally, although the electric-field effects on the photodetachment of H^- have a lot of experimental works [6–9] and theoretical calculations [10–14].

The *B*-spline-based complex-rotation method is used to investigate the electric field effects on He $(2,5a)$ and $(2,6a)$ $^1P^o$ and $^1D^e$ resonances in the photoionization from the He ground state. With a nearly complete set of finite L^2 basis functions, the *B*-spline-based configuration interaction (BSCI) basis has successfully applied to two-electron and divalent atoms [15]. On the other hand, recently the complex-rotation method has been used in the study of He ground-state photoionization [4,16] and the hydrogen atom in external electric or magnetic fields [17,18]. In the present investigation, we concentrate on the $(2,5a)$ and $(2,6a)$ $^1P^o$ states because the required field strengths for the phenomenon predicted in our work are very likely available in today's laboratories.

II. THEORY

A. BSCI basis for two-electron atoms

For two-electron atoms within the central-field approximation, the two-electron basis function $\psi^{\Lambda}_{n\ell,n'\ell'}(\mathbf{r_1},\mathbf{r_2})$ can be expressed as a sum of two-particle Slater-determinant wave functions over all magnetic quantum numbers in the form of [15]

$$\psi^{\Lambda}_{n\ell,n'\ell'}(\mathbf{r_1},\mathbf{r_2})=\sum_{\text{all } m\text{'s}}(-1)^{\ell'-\ell}[(2S+1)(2L+1)]^{1/2}\begin{pmatrix}\ell & \ell' & L\\ m & m' & -M_L\end{pmatrix}\begin{pmatrix}\frac{1}{2} & \frac{1}{2} & S\\ m_s & m_s' & -M_S\end{pmatrix}\phi^{mm_sm'm_s'}_{n\ell,n'\ell'}(\mathbf{r_1},\mathbf{r_2}), \tag{1}$$

where $\Lambda=(S,L,M_S,M_L)$ represents a set of quantum numbers S, L, M_S, and M_L. S is the total spin, L is the total orbital angular momentum, and M_S and M_L are the magnetic quantum numbers of S and L, respectively. The Slater-determinant wave function is constructed from the one-electron orbitals u_β, i.e.,

$$\phi^{mm_sm'm_s'}_{n\ell,n'\ell'}(\mathbf{r_1},\mathbf{r_2})=(2!)^{-1/2}\det|u_\beta(\mathbf{r_\mu})|, \tag{2}$$

and β represents the quantum numbers n_β, ℓ_β, m_β, and m_{s_β}, which define the one-electron orbital function. More specifically, $u_{n\ell mm_s}$ is given by the product of its spatial and spin parts, i.e.,

$$u_{n\ell mm_s}(\mathbf{r})=\frac{\chi_{n\ell}(r)}{r}Y_{\ell m}(\theta,\varphi)\sigma(m_s). \tag{3}$$

Note that the only component in the basis functions that is not predetermined is the radial part χ of the one-particle orbital function u.

The nonrelativistic radial functions $\chi_{n\ell}$ satisfy the eigenequation

$$h_\ell\chi_{n\ell}=\epsilon_{n\ell}\chi_{n\ell}. \tag{4}$$

The one-particle Hamiltonian in atomic unit is given by

$$h_\ell(r)=\left(-\frac{1}{2}\frac{d^2}{dr^2}-\frac{Z}{r}+\frac{1}{2}\frac{\ell(\ell+1)}{r^2}\right). \tag{5}$$

The solution $\chi_{n\ell}$ is expanded in terms of a set of *B* splines of order K and total number N defined between $r=0$ and $r=R$, i.e.,

$$\chi_{n\ell}(r)=\sum_{i=1}^{N}c_iB_i(r). \tag{6}$$

The index K is omitted from the functions B_i for simplicity.

B. Complex-rotation method

The Hamiltonian for two-electron atoms in an external field is [19]

$$H = T + V + \mathbf{F}\cdot\mathbf{r}, \tag{7}$$

where $\mathbf{F}$ is the external field and $\mathbf{r}=\mathbf{r}_1+\mathbf{r}_2$ is the position operator. The kinetic and potential operators in atomic units are given by

$$T = -\frac{1}{2}\nabla_1^2 - \frac{1}{2}\nabla_2^2 \tag{8}$$

and

$$V = -\frac{Z}{r_1} - \frac{Z}{r_2} + \frac{1}{r_{12}}, \tag{9}$$

respectively, where $r_{12}=|\mathbf{r}_1-\mathbf{r}_2|$ and Z is the nuclear charge. The field strength in atomic unit is 1 a.u.$=5.14\times10^9$ V/cm.

In the method of complex rotation, the radial coordinates are transformed by

$$r \rightarrow r e^{i\Theta}, \tag{10}$$

and the Hamiltonian can be written as

$$H(\Theta) = T e^{-2i\Theta} + V e^{-i\Theta} + \mathbf{F}\cdot\mathbf{r} e^{i\Theta}. \tag{11}$$

Complex eigenvalues are obtained by diagonalizing $H(\Theta)$ in a BSCI basis of real functions, and the complex resonance energy is given by

$$E_{\rm res} = E_r - i\Gamma/2. \tag{12}$$

The eigenstates of $H(\Theta)$ are normalized as [17,20]

$$H(\Theta)|\Psi_\nu(\Theta)\rangle = E_\nu(\Theta)|\Psi_\nu(\Theta)\rangle \tag{13}$$

and

$$\langle\overline{\Psi_\nu(\Theta)}|\Psi_\mu(\Theta)\rangle = \delta_{\nu\mu}, \tag{14}$$

where $\langle\overline{\Psi_\nu(\Theta)}|$ denotes the transposed value of $|\Psi_\nu(\Theta)\rangle$, not the Hermitian conjugate.

C. Photoionization cross sections

The photoionization cross section $\sigma(E)$ from the initial state $|\Psi_0\rangle$ with energy E_0 can be expressed in the dipole-length approximation as (in a.u.) [17,18]

$$\sigma^L(E) = 4\pi\alpha\Delta E\ \mathrm{Im}\sum_\nu \frac{\langle\overline{\Psi_\nu(\Theta)}|R(\Theta)D^L|\Psi_0\rangle^2}{E_\nu(\Theta)-E}, \tag{15}$$

where α is the fine-structure constant, $\Delta E = E - E_0$ is the transition energy, $D^L=\boldsymbol{\varepsilon}\cdot\mathbf{r}$ is the dipole-length operator for polarization $\boldsymbol{\varepsilon}$, and $R(\Theta)$ is the complex rotation operator given by [17]

$$R(\Theta) = \exp\left(-\Theta\frac{\mathbf{r}\cdot\mathbf{p}+\mathbf{p}\cdot\mathbf{r}}{2}\right). \tag{16}$$

The photoionization cross section can also be expressed in the dipole-velocity approximation as (in a.u.)

$$\sigma^V(E) = 4\pi\alpha\Delta E^{-1}\ \mathrm{Im}\sum_\nu \frac{\langle\overline{\Psi_\nu(\Theta)}|R(\Theta)D^V|\Psi_0\rangle^2}{E_\nu(\Theta)-E}, \tag{17}$$

where $D^V=\boldsymbol{\varepsilon}\cdot(\boldsymbol{\nabla}_1+\boldsymbol{\nabla}_2)$. Note that the complex-rotated Hamiltonian can be formally written as [17]

$$H(\Theta) = R(\Theta)HR(-\Theta). \tag{18}$$

Writing the complex dipole matrix into the real and imaginary parts as

$$\langle\overline{\Psi_\nu(\Theta)}|R(\Theta)D|\Psi_0\rangle = B_\nu + iC_\nu, \tag{19}$$

where $D=D^L$ and D^V in the length and velocity approximations, respectively, the photoionization cross section $\sigma(E)$ can then be parametrized and separated into nonresonant and resonant parts as [5,17]

$$\sigma(E) = \sigma_0(E) + \sum_\nu \sigma_\nu(E). \tag{20}$$

In Eq. (20), $\sigma_0(E)$ is the background cross section and $\sigma_\nu(E)$ is a modified Fano profile function for the νth resonance given by [16]

TABLE I. The calculated resonant energies E_r (in a.u.), widths Γ (in a.u.), Fano q parameters, and the fitted background cross sections $\sigma_0(E)$ and σ_0 (in Mb) of the He $(2,5a)\,{}^1P^o$ and ${}^1D^e$ resonances for the parametrized $\sigma(E)$, as defined by Eq. (24). The weakly energy-dependent $\sigma_0(E)$ is expressed in a linear fit as a function of energy E in a.u., i.e., $\sigma_0(E)=a+bE$. The electric-field strengths F are in atomic units. Numbers in square brackets indicate powers of 10.

	$(2,5a)\,{}^1P^o$				$(2,5a)\,{}^1D^e$				$\sigma_0(E)$	
F	E_r	Γ	q	σ_b	E_r	Γ	q	σ_b	a	b
0	−0.521 450	6.56[−5]	−2.88	1.086	−0.522 646	1.29[−4]			9.21	15.48
2.5[−5]	−0.521 566	5.97[−5]	−2.86	1.083	−0.522 707	1.24[−4]	−2.80	3.6[−3]	11.55	19.94
5.0[−5]	−0.521 885	4.72[−5]	−2.81	1.052	−0.522 875	1.11[−4]	−2.83	0.016	18.57	33.32
7.5[−5]	−0.522 339	3.62[−5]	−2.75	0.939	−0.523 122	9.34[−5]	−2.86	0.042	28.89	53.04
1.0[−4]	−0.522 880	2.88[−5]	−2.67	0.700	−0.523 426	7.47[−5]	−2.87	0.096	14.79	26.04
1.25[−4]	−0.523 465	2.25[−5]	−2.40	0.298	−0.523 786	5.89[−5]	−2.81	0.209	17.74	31.64
1.5[−4]	−0.523 969	1.56[−5]	−9.74	3.3[−3]	−0.524 315	5.31[−5]	−2.48	0.230	27.01	49.32

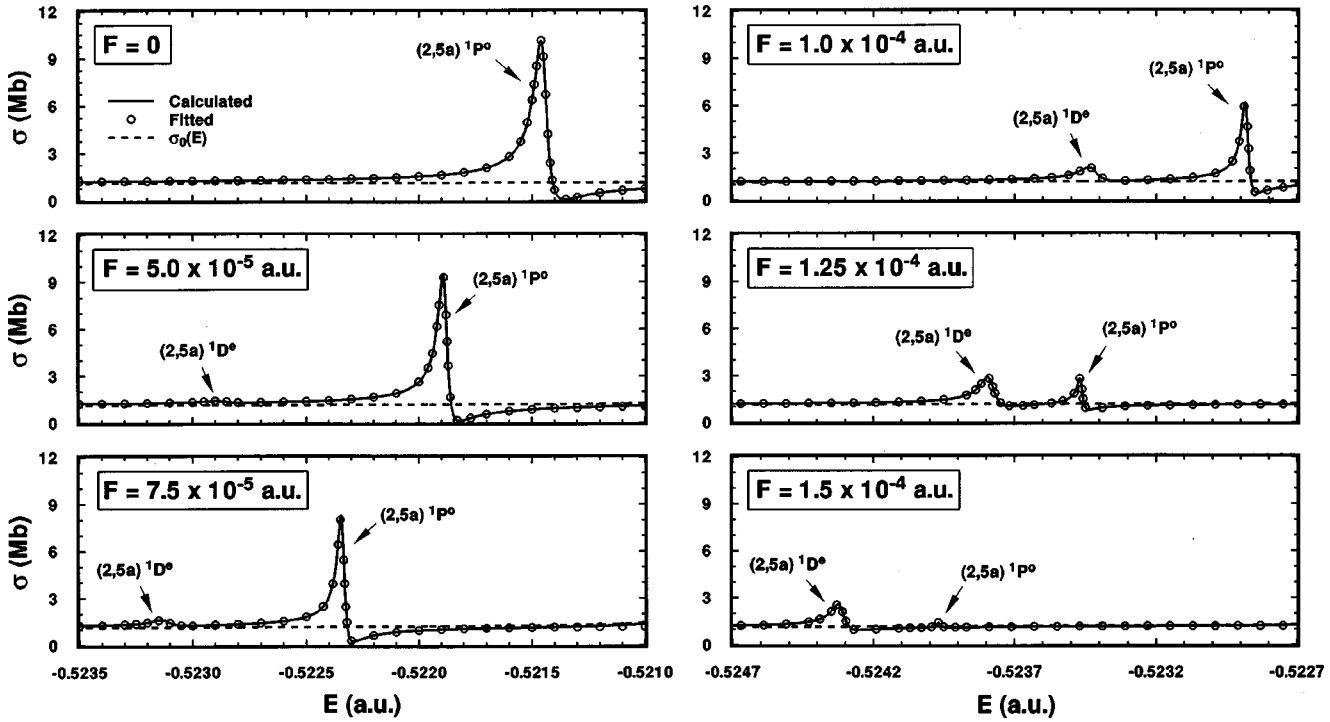

FIG. 1. Electric-field effects on the He ground-state photoionization in the energy region of the $(2,5a)\,^1P^o$ resonance at a field strength F varying from 0 to 1.5×10^{-4} a.u. The vertical scale is kept uniform. The solid lines are our calculated photoionization spectra using Eq. (17). The fitted results in open circles are obtained directly from the parametrized $\sigma(E)$ defined by Eq. (24) with the parameters given in Table I. The calculated background cross sections $\sigma_0(E)$ in Eq. (24) are also shown as dashed lines.

$$\sigma_\nu(E)=\sigma_b^\nu\left[\frac{(q_\nu+\varepsilon_\nu)^2}{(1+\varepsilon_\nu^2)}-1\right], \tag{21}$$

where

$$\varepsilon_\nu=(E-E_\nu)/\tfrac{1}{2}\Gamma_\nu \quad \text{(reduced energy)},$$

$$q_\nu=-\frac{B_\nu}{C_\nu} \quad \text{(Fano } q \text{ parameter)}, \tag{22}$$

$$\sigma_b^\nu=8\pi\alpha g(E)\frac{C_\nu^2}{\Gamma_\nu} \quad \text{(background)},$$

where E_ν and Γ_ν are the resonant energy and width of the νth resonance, and $g(E)=\Delta E$ and ΔE^{-1} in the length and velocity approximations, respectively. If q_ν, Γ_ν, and σ_b^ν can be regarded as independent of E over a sufficient range [21], the resonant strength S_ν of the νth resonance can be defined as [16,21]

$$S_\nu=\int_{-\infty}^{+\infty}dE\,\sigma_\nu(E)=\frac{\pi}{2}\sigma_b^\nu\Gamma_\nu(q_\nu^2-1); \tag{23}$$

i.e., S_ν gives the area under the modified Fano profile function σ_ν of the νth resonance.

III. CALCULATIONS AND RESULTS

In the presence of an electric field, M_L remains a good quantum number. For a linearly polarized light with the direction of polarization parallel to the electric field, the $M_L=0$ components of resonant states could be excited from the $^1S^e$ ground state. Angular-momentum states with $^1S^e$, $^1P^o$, $^1D^e$, and $^1F^o$ are coupled together to form a BSCI basis of 3680 configurations by the external electric field for the $M_L=0$ components. We first investigate the He $(2,5a)\,^1P^o$ resonant state and a nearby $(2,5a)\,^1D^e$ state. For the field-free case, the resonant energy and width for the $(2,5a)\,^1P^o$ state are $E_r=-0.521\,450$ a.u. and $\Gamma=6.56\times10^{-5}$ a.u., in good agreement with $E_r=-521\,489$ a.u. and $\Gamma=6.58\times10^{-5}$ a.u. [22]. They are also comparable to $E_r=-0.521\,500$ a.u. and $\Gamma=6.05\times10^{-5}$ a.u. given in Ref. [5]. As for the $(2,5a)\,^1D^e$ state, the resonant energy and width are $E_r=-0.522\,646$ a.u. and $\Gamma=1.29\times10^{-4}$ a.u., which are comparable to $E_r=-0.522\,72$ a.u. and $\Gamma=1.19\times10^{-4}$ a.u. [22].

In a rigorous theoretical approach, not only the final state,

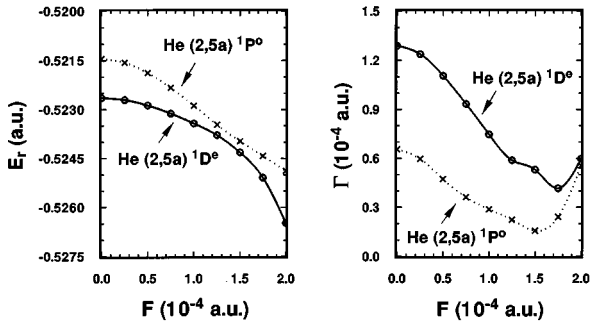

FIG. 2. Electric-field effects on the resonant energies and widths of He $(2,5a)\,^1P^o$ and $(2,5a)\,^1D^e$ states. The spline fits are used to connect the calculated data points.

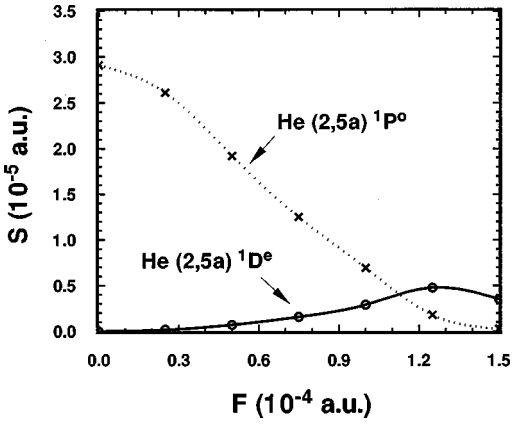

FIG. 3. Field variations on the resonant strength S of He $(2,5a)\,{}^1P^o$ and $(2,5a)\,{}^1D^e$ states, where S is defined by Eq. (23). The spline fits are used to connect the calculated data points.

but also the initial $^1S^e$ ground state should be obtained by the diagonalization of the Hamiltonian with the external electric field to account for the tunneling effects induced by the electric field. However, our calculations have shown that, after the Stark mixing, the ground state is still nearly a pure $^1S^e$ state for all the electric-field strengths under the present investigation. Therefore the tunneling effect for the ground state in the presence of an electric field can be ignored. In the present calculation, a BSCI basis of 3860 configurations is used for the strongly correlated He $^1S^e$ ground state. Since the agreement between the length and velocity results is better than 5%, only velocity results are shown throughout this paper.

In the energy region around the He $(2,5a)\,{}^1P^o$ and $(2,5a)\,{}^1D^e$ resonances, the parametrized $\sigma(E)$ defined by Eq. (20) can be simplified as

$$\sigma(E)=\sigma_0(E)+\sum_{\nu=1}^{2}\sigma_b^{\nu}\left[\frac{(q_\nu+\varepsilon_\nu)^2}{(1+\varepsilon_\nu^2)}-1\right], \tag{24}$$

where the sum over the resonance index ν is limited to the $(2,5a)\,{}^1P^o$ and $(2,5a)\,{}^1D^e$ states. Note that the resonant energy E_ν and width Γ_ν of a state ν in the reduced energy $\varepsilon_\nu=(E-E_\nu)/\frac{1}{2}\Gamma_\nu$ are obtained directly from the complex eigenvalue $E_\nu(\Theta)=E_\nu-i\Gamma_\nu/2$, and the Fano q parameter q_ν can be calculated using Eq. (22). The weakly energy-dependent background cross sections $\sigma_0(E)$ and σ_b^ν are determined by a linear and a constant fit, respectively. Table I lists all the parameters for the parametrized $\sigma(E)$ defined by Eq. (24), including the calculated resonant energies E_r, widths Γ, Fano q parameters, and the fitted background cross sections $\sigma_0(E)$ and σ_b. Figure 1 presents the electric-field effects on the resonant structures for the He $(2,5a)\,{}^1P^o$ and $(2,5a)\,{}^1D^e$ states. The solid lines are our calculated photoionization spectra using Eq. (17). For a given energy region, about 1000 data points are used to construct the solid curve. The open circles are the parametrized $\sigma(E)$ obtained by using Eq. (24). The calculated background cross section $\sigma_0(E)$ in Eq. (24) is also given in Fig. 1, and as expected, it is indeed weakly energy dependent. The agreement between the parametrized $\sigma(E)$ and the calculated one is nearly perfect. In the absence of an electric field, only the $^1P^o$ state can be accessed from the He $^1S^e$ ground state by single-photon absorption. When the external electric field is turned on, the

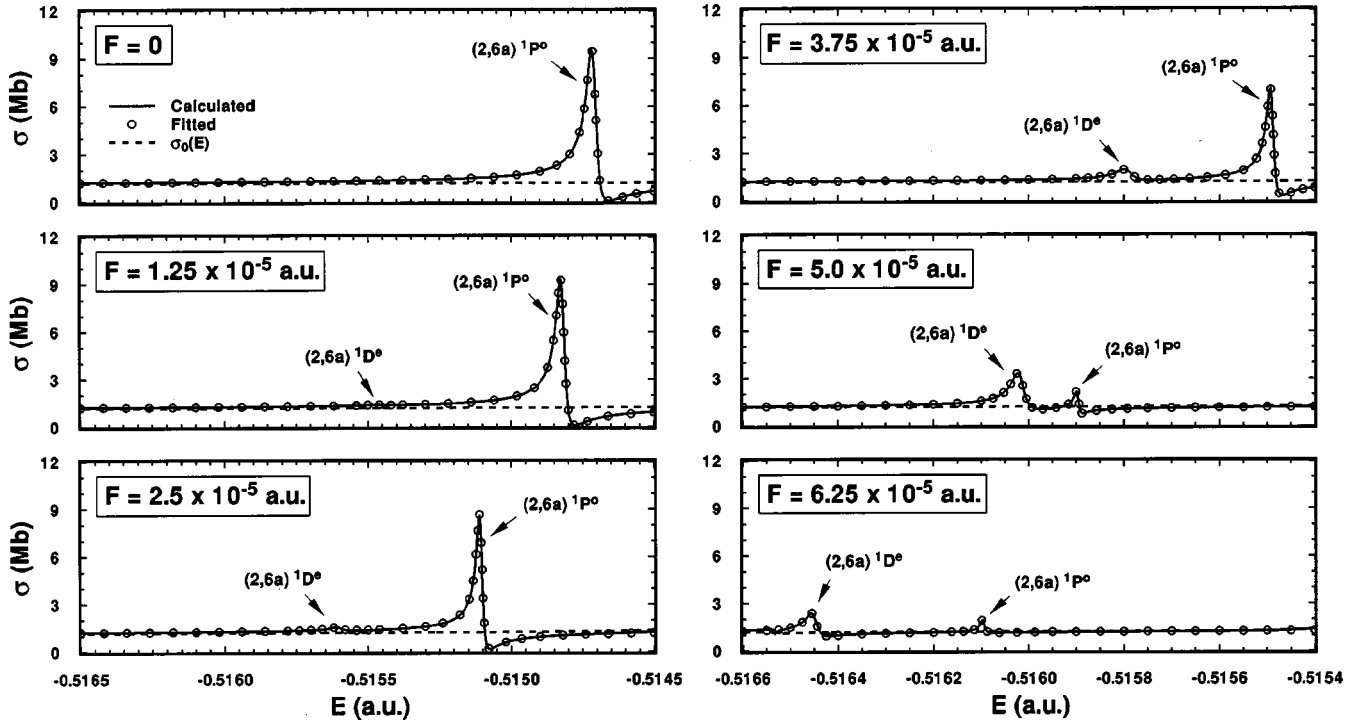

FIG. 4. Electric-field effects on the He ground-state photoionization in the energy region of the $(2,6a)\,{}^1P^o$ resonance at a field strength F varying from 0 to 6.25×10^{-5} a.u. The vertical scale is kept uniform. The solid lines are our calculated photoionization spectra using Eq. (17). The fitted results in open circles are obtained directly from the parametrized $\sigma(E)$ defined by Eq. (24) with the parameters given in Table II. The calculated background cross sections $\sigma_0(E)$ in Eq. (24) are also shown as dashed lines.

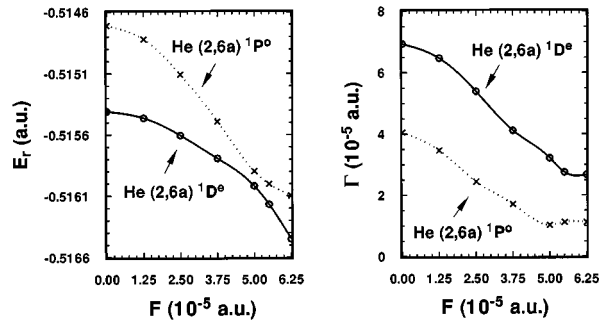

FIG. 5. Electric-field effects on the resonant energies and widths of He $(2,6a)\,{}^1P^o$ and $(2,6a)\,{}^1D^e$ states. The spline fits are used to connect the calculated data points.

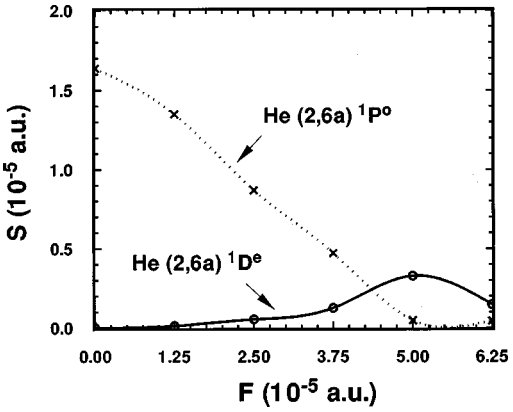

FIG. 6. Field variations on the resonant strength S of He $(2,6a)\,{}^1P^o$ and $(2,6a)\,{}^1D^e$ states, where S is defined by Eq. (23). The spline fits are used to connect the calculated data points.

nearby $^1D^e$ resonance is induced by the $^1P^o$ state due to the Stark mixing of these two resonances. The magnitude of the $^1D^e$ resonance increases for increasing electric-field strength, and the magnitude of the $^1P^o$ resonance decreases when the field strength is increased. Eventually, the $^1P^o$ resonance is practically quenched at about $F=1.5\times10^{-4}$ a.u. As for the $^1D^e$ state, its magnitude is first increased for increasing field strength until $F=1.25\times10^{-4}$ a.u. approximately. After that, the quenching effect is also applied to the $^1D^e$ state when the field strength is further increased.

Figure 2 shows the changes of resonant energies and widths of He $(2,5a)\,{}^1P^o$ and $(2,5a)\,{}^1D^e$ states, where spline fits are used to connect the calculated data points. Initially, when the external electric field is turned on, the resonant energies start to shift downward for both the $^1P^o$ and $^1D^e$ states due to the *quadratic Stark effect* [23,24], and the energy separation between them becomes smaller. When they reach the avoided crossing at about $F=1.25\times10^{-4}$ a.u., the $^1D^e$ state by then has about the same maximum cross section as the $^1P^o$ state through the redistribution of magnitude as shown earlier in Fig. 1. After passing the avoided crossing, the resonant energies are shifted downward all the way. As for the resonant widths, it is seen that initially when the field strength is increased, the widths start to decrease as a result of losing autoionization intensities to other singlet-spin states [24]. The identification of such states is outside the scope of our present investigation. Nevertheless, it is an outstanding question which should be studied in the future. The widths reach minima at critical field strengths F_c at about $F_c=1.5\times10^{-4}$ and 1.75×10^{-4} a.u. for the $^1P^o$ and $^1D^e$ states, respectively, and start to increase as F is further increased. Before the field reaches such a critical strength F_c, the external field is not strong enough to break the *two-electron bonding* due to the strong correlation effects of the two doubly excited electrons. The external field in the weak field cases simply acts as a mixing agent for the pair and other neighboring states, resulting in the decrease of widths for the $^1P^o$ and $^1D^e$ pair, as was discussed earlier in the text. Once the field strength reaches a critical value F_c, the *two-electron bonding* is broken by the external field; the one-electron tunneling effect then starts to dominate the autoionization processes. At the high-field region, the widths start to increase in a more rapid fashion. Such a phenomenon is due to the fact that the effective potential barrier, formed by the combination of the atomic potential and the external dc field, would become narrower as the external electric-field strength increases further. The time required for an electron to tunnel out of the potential barrier would therefore be shorter, resulting in the broadening of the autoionization width in the high-field region [25].

Detailed field variations of the resonant strength S of the He $(2,5a)\,{}^1P^o$ and $^1D^e$ states are shown in Fig. 3. Again, the spline fits are used to connect the calculated data points. It can be seen that the $^1D^e$ state attains the maximum resonant strength at the avoided crossing near $F=1.25\times10^{-4}$ a.u., which further suggests that the strongest Stark interaction

TABLE II. The calculated resonant energies E_r (in a.u.), widths Γ (in a.u.), Fano q parameters, and the fitted background cross sections $\sigma_0(E)$ and σ_0 (in Mb) of the He $(2,6a)\,{}^1P^o$ and $^1D^e$ resonances for the parametrized $\sigma(E)$, as defined by Eq. (24). The weakly energy-dependent $\sigma_0(E)$ is expressed in a linear fit as a function of energy E in a.u., i.e., $\sigma_0(E)=a+bE$. The electric-field strengths F are in atomic units. Numbers in square brackets indicate powers of 10.

	$(2,6a)\,{}^1P^o$				$(2,6a)\,{}^1D^e$				$\sigma_0(E)$	
F	E_r	Γ	q	σ_b	E_r	Γ	q	σ_b	a	b
0	−0.514 710	4.05[−5]	−2.71	1.135	−0.515 408	6.94[−5]			13.44	23.79
1.25[−5]	−0.514 821	3.46[−5]	−2.67	1.133	−0.515 462	6.47[−5]	−3.00	4.5[−3]	19.97	36.43
2.5[−5]	−0.515 107	2.44[−5]	−2.63	1.074	−0.515 604	5.39[−5]	−3.01	0.022	38.04	71.42
3.75[−5]	−0.515 490	1.70[−5]	−2.58	0.875	−0.515 792	4.11[−5]	−2.98	0.069	27.73	51.41
5.0[−5]	−0.515 896	1.02[−5]	−1.98	0.284	−0.516 017	3.21[−5]	−2.87	0.251	37.44	70.22
6.25[−5]	−0.516 097	1.11[−5]	−4.41	0.039	−0.516 450	2.67[−5]	−2.31	0.227	72.45	138.1

between the $^1P^o$ and $^1D^e$ states is occurred at the avoided crossing.

A similar Stark effect between the $^1P^o$ and $^1D^e$ states is also found in the other $(2,na)$ pairs, such as in the energy region of the $(2,6a)\,^1P^o$ resonance shown in Figs. 4–6 and Table II. For the field-free case, the resonant energy and width for the $(2,6a)\,^1P^o$ state are $E_r=-0.514\,711$ a.u. and $\Gamma=4.05\times10^{-5}$ a.u., which are comparable to $E_r=-0.514\,72$ a.u. and $\Gamma=3.8\times10^{-5}$ a.u. [22]. As for the $(2,6a)\,^1D^e$ state, the resonant energy and width are $E_r=-0.515\,409$ a.u. and $\Gamma=6.94\times10^{-5}$ a.u., which are comparable to $E_r=-0.515\,435$ a.u. and $\Gamma=6.8\times10^{-5}$ a.u. [22]. The magnitude and resonant strength of the $^1P^o$ state are found to decrease when the field strength is first turned on, and eventually it is practically quenched at about $F=6.25\times10^{-5}$ a.u.($\sim$321 kV/cm). As for the nearby $^1D^e$ state, its magnitude and resonant strength are first found to increase to the avoided crossing at about $F=5.0\times10^{-5}$ a.u. After that, its magnitude and resonant strength are also found to be diminished as the field strength is increased further.

In summary, we have carried out a theoretical investigation of strong electric-field effects on the He$(2,5a)$ and $(2,6a)\,^1P^o$ and $^1D^e$ resonances. Our findings hopefully will stimulate experimental activities to investigate such an interesting phenomenon.

ACKNOWLEDGMENTS

This work was supported by the Academia Sinica and the National Science Council. The authors would like to thank Professor T. N. Chang and Professor K. T. Chung for many useful discussions.

[1] M. Domke, G. Remmers, and G. Kaindl, Phys. Rev. Lett. **69**, 1171 (1992); M. Domke, K. Schulz, G. Remmers, G. Kaindl, and D. Wintgen, Phys. Rev. A **53**, 1424 (1996).
[2] K. Schulz, G. Kaindl, M. Domke, J. D. Bozek, P. A. Heimann, A. S. Schlachter, and J. M. Rost, Phys. Rev. Lett. **77**, 3086 (1996).
[3] R. Moccia and S. Spizzo, Phys. Rev. A **43**, 2199 (1991).
[4] D. Wintgen and D. Delande, J. Phys. B **26**, L399 (1993).
[5] T. K. Fang and T. N. Chang, Phys. Rev. A **56**, 1650 (1997).
[6] P. A. M. Gram, J. C. Pratt, M. A. Yates-Williams, H. C. Bryant, J. Donahue, H. Sharifian, and H. Tootoonchi, Phys. Rev. Lett. **40**, 107 (1978).
[7] H. C. Bryant, D. A. Clark, K. B. Butterfield, C. A. Frost, J. B. Donahue, P. A. M. Gram, M. E. Hamm, R. W. Hamm, J. C. Pratt, M. Y. Yates, and W. W. Smith, Phys. Rev. A **27**, 2889 (1983).
[8] S. Cohen, H. C. Bryant, C. J. Harvey, J. E. Stewart, K. B. Butterfield, D. A. Clark, J. B. Donahue, D. W. MacArthur, G. Comtet, and W. W. Smith, Phys. Rev. A **36**, 4728 (1987).
[9] P. G. Harris, H. C. Bryant, A. H. Mohagheghi, C. Tang, J. B. Donahue, C. R. Quick, R. A. Reeder, S. Cohen, W. W. Smith, J. E. Stewart, and C. Johnstone, Phys. Rev. A **41**, 5968 (1990).
[10] A. R. P. Rau and H. Wong, Phys. Rev. A **37**, 632 (1988).
[11] M. L. Du and J. B. Delos, Phys. Rev. A **38**, 5609 (1988).
[12] B. Gao and A. F. Starace, Phys. Rev. A **42**, 5580 (1990).
[13] N. Y. Du, I. I. Fabrikant, and A. F. Starace, Phys. Rev. A **48**, 2968 (1993).
[14] H. Bachau and F. Martin, J. Phys. B **29**, 1451 (1996).
[15] T. N. Chang, in *Many-body Theory of Atomic Structure and Photoionization*, edited by T. N. Chang (World Scientific, Singapore, 1993), p. 213.
[16] J. M. Rost, K. Schulz, M. Domke, and G. Kaindl, J. Phys. B **30**, 4663 (1997).
[17] A. Buchleitner, B. Grémaud, and D. Delande, J. Phys. B **27**, 2663 (1994).
[18] D. Delande, A. Bommier, and J. C. Gay, Phys. Rev. Lett. **66**, 141 (1991).
[19] Y. K. Ho, Phys. Rep. **99**, 1 (1983).
[20] T. N. Rescigno and V. McKoy, Phys. Rev. A **12**, 522 (1975).
[21] U. Fano, Phys. Rev. **124**, 1866 (1961).
[22] D. H. Oza, Phys. Rev. A **33**, 824 (1986).
[23] H. Friedrich, *Theoretical Atomic Physics* (Springer-Verlag, Berlin, 1991).
[24] Y. K. Ho, J. Korean Phys. Soc. **32**, 224 (1998).
[25] Y. K. Ho, Chin. J. Phys. **34**, 1136 (1996); Z. Phys. D **38**, 191 (1996).